Published in final edited form as:

Arterioscler Thromb Vasc Biol. 2015 September ; 35(9): 1920–1927. doi:10.1161/ATVBAHA.115.305747.

Targeted Knockdown of Hepatic SOAT2 with Antisense Oligonucleotides Stabilizes Atherosclerotic Plaque in ApoB100-only LDLr$^{-/-}$ Mice

John T. Melchior[1], **John D. Olson**[2], **Kathryn L. Kelley**[1], **Martha D. Wilson**[1], **Janet K. Sawyer**[1], **Kerry M. Link**[2], and **Lawrence L. Rudel**[1]

[1]Department of Pathology, Section on Lipid Sciences, Wake Forest University Health Sciences, Winston-Salem, North Carolina, USA

[2]Center for Biomolecular Imaging, Wake Forest University Health Sciences, Winston-Salem, North Carolina, USA

Abstract

Objective—To test the hypothesis that the attenuation of CO packaging into apoB-containing lipoproteins will arrest progression of pre-existing atherosclerotic lesions.

Approach and Results—Atherosclerosis was induced in apoB-100 only, LDLr$^{-/-}$ mice by feeding a diet enriched in cis-monounsaturated fatty acids (cis-MUFAs) for 24 weeks. A subset of mice was then sacrificed to quantify the extent of atherosclerosis. The remaining mice were continued on the same diet (controls) or assigned to the following treatments for 16 weeks: (1) a diet enriched in n-3 polyunsaturated fatty acids, (2) the cis-MUFA diet plus bi-weekly injections of an antisense oligonucleotide (ASO) specific to hepatic SOAT2; or (3) the cis-MUFA diet and bi-weekly injections of a non-targeting hepatic ASO. Extent of atherosclerotic lesions in the aorta was monitored morphometrically *in vivo* with magnetic resonance imaging (MRI) and *ex vivo* histologically and immunochemically. Hepatic knockdown of SOAT2 via ASO treatment arrested lesion growth and stabilized lesions.

Conclusions—Hepatic knockdown of SOAT2 in apoB100-only, LDLr$^{-/-}$ mice resulted in remodeling of aortic atherosclerotic lesions into a stable phenotype, suggesting SOAT2 is a viable target for treatment of atherosclerosis.

Keywords

Atherosclerosis; magnetic resonance imaging; cholesterol; lipids and lipoproteins; remodeling

Address correspondence to: Dr. L.L. Rudel, Wake Forest University Health Sciences, Department of Pathology, Section on Lipid Sciences, Medical Center Blvd, Winston-Salem, NC 25157-1040. Tel: 336-716-2823 Fax: 336-716-6279 lrudel@wakehealth.edu.

DISCLOSURES

None

INTRODUCTION

Disruption of unstable atherosclerotic plaques accounts for most acute clinical events associated with coronary heart disease (CHD)[1]. Imbalance in vascular lipid homeostasis results in lipid deposition in the artery wall, a primary feature of atherosclerosis. Lipid accounts for over 40% of the cross-sectional area in lesions with a high propensity to rupture[2]. Thus, it is of interest to identify targets that reduce lipid content in atherosclerotic lesions and favor remodeling into a more stable plaque phenotype.

Studies of atherosclerosis in humans[3, 4] and animal models[5] suggest that at least in part, robust reductions in circulating levels of apoB-containing lipoproteins are required to favorably remodel the plaque. Understudied, but also potentially important, are interventions that reduce the cholesterol oleate content of plasma apoB-containing lipoproteins, which limit the development of atherosclerotic lesions. A body of evidence indicates that cholesterol oleate (CO) is an important factor in the pathobiology of atherosclerosis. For instance, in the Atherosclerosis Risk in Communities (ARIC) study, Ma et al. showed that carotid artery wall intima-media thickness (IMT) was positively associated with plasma CO levels[6]. Moreover, the Uppsala Longitudinal Study of Adult Men showed a positive association between death from cardiovascular disease and plasma CO concentrations[7]. Studies in nonhuman primates have shown that core enrichment of low-density lipoproteins (LDLs) with CO is strongly and positively associated with more severe coronary artery atherosclerosis[8, 9].

Steroyl O-acyltransferase 2 (SOAT2), an enzyme bound to the endoplasmic reticulum in hepatocytes and enterocytes, catalyzes the formation of CO from fatty acyl-CoA and free cholesterol. Genetic deletion or knockdown of SOAT2 in mice inhibits packaging of CO into apoB-containing lipoproteins and protects against atherogenesis[10, 11]. Dietary studies, in which availability of the preferred substrate of SOAT2, monoacyl-CoA was limited, also showed reduced CO packaging into apoB-containing lipoprotein particles and atheroprotection in nonhuman primates[9] and mouse models of atherosclerosis[11, 12].

Despite the strong evidence that inhibition of SOAT2 prevents atherosclerosis, it is unknown whether SOAT2 inhibition could treat established atherosclerotic lesions. In the present study, we hypothesized that reducing CO content of apoB-containing lipoproteins via SOAT2 inhibition would promote regression of lipid-rich atherosclerotic lesions in apoB-100 only $LDLr^{-/-}$ mice. To inhibit SOAT2, we used an antisense oligonucleotide (ASO) to specifically knock down gene expression of SOAT2 in the liver. A novel magnetic resonance imaging (MRI) protocol was developed to measure changes in the wall of the aortic arch in mice. Hepatic knockdown of SOAT2 arrested aortic lesion growth and resulted in a plaque composition consistent with a more stable phenotype, suggesting that SOAT2 could be a valuable therapeutic target for the treatment of atherosclerosis.

METHODS

Materials and Methods are available in the online-only data supplement.

RESULTS

MRI can monitor changes in aortic wall area in vivo

One aim of this study was to evaluate MRI as a tool to monitor temporal changes in atherosclerosis *in vivo*. Thus, we developed a technique to capture transverse images of the aorta at a resolution of 59 X 59 X 250 μm^3, a high degree of *in vivo* voxel resolution. To assess the accuracy of the technique, transverse MR images were directly compared to *ex vivo* histologic sections from the same region of the aorta. Aortic morphology on MR images showed excellent agreement with histological sections from both Period 1 (Figure 1A) and Period 2 (Figure 1B). Using both methods, we observed eccentric thickening of the aorta on the ventral side of the vessel during lesion development; a finding consistent with previous reports that lesion formation in $LDLr^{-/-}$ mice occurs at the lesser curvature of the arch[13].

Using MRI, we measured aortic wall area by manually tracing the outside and inside borders of the vessel (Figure 1C). Areas occupied within the outside and inside borders were defined as the outer wall area and lumen cross-sectional areas, respectively, and the difference between the two was defined as the cross-sectional area of the vessel wall. Cross-sectional wall area measurements were compared between MRI and histologically stained sections. A regression analysis (Figure 1D) showed a strong relationship between the values obtained from either method (R^2=0.75, P<0.0001). The relationship was further assessed by generating a Bland-Altman plot (Figure 1E), to determine systematic differences between two measurement techniques. The overall mean difference in values obtained between the two methods was 0.9 mm^2. All data points fell within the limits of agreement (mean difference ± 1.96 SD), indicating the two methodologies can be used interchangeably for monitoring changes in arterial wall morphometry.

SOAT2 ASO treatment results in smaller atherosclerotic lesions in vivo

Transverse MR images were obtained throughout each period of the study; we averaged values for each mouse from at least 3 MR images per mouse. Figure 2 illustrates the morphometric changes in the artery wall over time. Wall area increased in both diet groups during Period 1 (Figure 2C); however, the cis-MUFA group had accelerated wall growth compared to n-3 PUFA animals after 12 and 24 weeks on diet. As an additional measurement of atherosclerosis burden, we normalized wall area to outer wall area as an approximate evaluation of lesion encroachment into the lumen (Figure 2D). The cis-MUFA-fed group showed increased encroachment at both 12 and 24 weeks of treatment compared to the n-3 PUFA-fed group. This accelerated lesion development is consistent with previous reports in apoB-100, $LDLr^{-/-}$ mice using the same experimental diets[11, 14].

Changes in arterial morphometry for Period 2 are shown in Figure 2E–H. Wall area increased during the first 12 weeks of Period 2 in all three experimental groups (Figure 2G). However, at 16 weeks, wall area was significantly reduced in the SOAT2 ASO group versus the cis-MUFA and n-3 PUFA groups. Furthermore, after 16 weeks, SOAT2 ASO-treated mice had reduced encroachment indicative of lesion reduction.

SOAT2 ASO-treated mice have less aortic atherosclerosis and accelerated plaque stabilization

We evaluated atherosclerosis histologically and chemically at the end of Period 2 and compared treatment groups with cis-MUFA mice sacrificed at the end of Period 1. Histologic sections of the aortic arch were stained with VVG and morphometrically assessed. Measurements were obtained in a subset of 4 mice per group after averaging 4 or more cross-sections per mouse (see Supplemental Table I). Intimal area was measured and used as the morphometric evaluation of atherosclerotic burden. Intimal area increased in all experimental groups at the end of Period 2; however, SOAT2 ASO-treated mice had the smallest increase and were not statistically different from cis-MUFA mice sacrificed at the end of Period 1.

Lipid and collagen content, markers of lesion stability[15, 16], were evaluated from slides stained with Oil-Red-O (ORO) for lipid or Masson's trichrome (MT) for collagen. Representative stained sections from each group are included in Supplemental Figure IV. Sections from the SOAT2 ASO-treated group had less lipid (14.3% vs 1.4%) but more collagen (10.9% vs 29.6%) compared to Period 1 cis-MUFA-fed mice (Figures 3B, 3C). Although no statistically significant differences were found in the n-3 PUFA-treated group after Period 2 compared to the cis-MUFA group after Period 1, results showed a trend similar to SOAT2 ASO treatment. To further investigate plaque stability, we calculated the ratio of lipid to collagen; lower ratios indicated a more stable lesion. The cis-MUFA-fed group at Period 2 had the highest ratio (0.29), followed by the n-3 PUFA-fed group at Period 2 (0.25); the SOAT2 ASO-treated group had the lowest ratio (0.05).

We then measured cholesterol ester and free cholesterol content in the abdominal aorta distal to the aortic arch (Figures 3D, 3E). The control group had the largest increase (over twofold) in CE deposition in the artery wall after 24 weeks of diet. Mice receiving the n-3 PUFA diet during Period 2 also had significantly more CE deposition into the artery wall compared to mice consuming the cis-MUFA diet in Period 1. Mice receiving SOAT2 ASO had no additional CE accumulation in the abdominal aorta after 16 weeks of treatment. FC was significantly elevated in all groups at Period 2 compared to control mice after Period 1.

Plasma lipoprotein concentrations are attenuated in mice treated with n-3 PUFAs and SOAT2 ASO

Previous studies in this model have shown that diet composition and expression of SOAT2 can influence plasma lipoprotein concentrations[10, 11, 14]. Figure 4 shows the total plasma cholesterol (TPC) response (Figure 4A) and cholesterol distribution among lipoproteins (Figure 4B–C) during the study. TPC in control mice fed the cis-MUFA diet increased from 370 mg/dl to 1,536 mg/dl over 24 weeks, mostly attributable to large increases in the apoB-containing very-low and low-density lipoproteins (VLDL and LDL). Most of the increase (64%) occurred in the LDL fraction. There was a small (~18 mg/dl) but significant elevation in high-density lipoprotein (HDL) concentrations, which accounted for about 1% of the increase in TPC. In contrast, the TPC and cholesterol concentrations in n-3 PUFA-fed mice remained at or near baseline values throughout Period 1.

During Period 2, a modest, but non-significant decrease in TPC was observed in the cis-MUFA-fed group. Large decreases in TPC were observed in the n-3 PUFA-fed (decrease of 874 mg/dl) and SOAT2 ASO-fed (982 mg/dl) groups after 16 weeks. Most of the decrease in both groups was attributable to reductions in the apoB-containing lipoproteins. In the n-3 PUFA-fed group, VLDL contributed ~40% of the decrease and LDL contributed ~ 60% of the decrease. HDL remained unchanged after 16 weeks of treatment. In the SOAT2 ASO-treated group, LDL accounted for 61% of the decrease in TPC, whereas VLDL accounted for (37% of the decrease. Although HDL only accounted for 2% of the decrease in TPC in the SOAT2 ASO-treated group, there was a nearly 2-fold reduction within the HDL fraction (to 26.7 mg/dl) after 16 weeks of SOAT2 ASO treatment.

LDL composition is altered in mice treated with n-3 PUFAs and SOAT2 ASO

LDL was isolated from plasma by ultracentrifugation; compositional differences among experimental groups are summarized in Supplemental Table II. Each constituent is expressed as a percentage of the LDL particle. No compositional differences were observed in LDLs from cis-MUFA mice in either Period 1 or 2. At the end of Period 2, both n-3 PUFA and SOAT2 ASO-treated mice had compositional differences in LDL surface constituents and increased protein and decreased detectable PL, compared to cis-MUFA mice sacrificed at the end of Period 1. Additionally, the n-3 PUFA Period 2 mice had LDLs with an increase in FC. Alterations in LDL core constituents were only observed in SOAT2 ASO-treated mice in Period 2; they had an increase in percentage of core TG and a trend towards decreased core CE percentage (P=0.054).

Individual LDL CEs were quantified by mass spectrometry; percentages based on individual fatty acid components are shown in Table 1. Dietary fat type significantly altered the CE species of the LDL core during Period 1. Although LDL CEs from both experimental diet groups contained primarily monounsaturated fatty acids (45–50%), the primary differences observed in CEs between the two groups were in polyunsaturated fatty acids. n-3 and n-6 polyunsaturated fatty acids contributed 7% and 36%, respectively, of the LDL CE fraction in the cis-MUFA-fed group. In the n-3 PUFA group, n-3 and n-6 polyunsaturated fatty acids contributed 36% and 16%, respectively, of the LDL CE fraction. Within the monounsaturated CEs, the primary difference between the two groups was observed in CO (%18:1). CO contributed 38% of the CE fraction in the cis-MUFA group and 25% in the n-3 PUFA group.

In Period 2, no differences in fatty acid composition were observed in the cis-MUFA-fed group, but both the n-3 PUFA-fed and SOAT2 ASO-treated mice had significantly altered CE species in the LDL core. Dietary treatment with n-3 PUFAs reduced monounsaturated CEs by 8%. The primary differences observed in the n-3 PUFA group were in the amounts of n-3 and n-6 polyunsaturated fatty acids in the CE core. After the 16 weeks of treatment, n-3 polyunsaturated fatty acids increased from 7% to 35% and n-6 polyunsaturated fatty acids decreased from 36% to 16%. In comparison, SOAT2 ASO significantly reduced the amount of monounsaturated CEs in the LDL (from 51% to 15%), increased n-3 polyunsaturated CEs from 7% to 14%, and increased n-6 polyunsaturated CEs from 36% to 68%. Both the n-3 PUFA-fed and SOAT2 ASO-treated mice had a reduction in CO content

in LDL. CO comprised 38% of the CE fraction prior to treatment. Dietary treatment with n-3 PUFAs reduced CO to 25% and SOAT2 ASO reduced CO to 10%.

LDL CE composition is associated with severity of atherosclerosis

We had hypothesized that eliminating the atherogenic insult (i.e. LDL enriched in CO) could facilitate plaque resolution. Figure 5 highlights the relationship between the CO enrichment of the LDL and atherosclerosis as evaluated *in vivo* by MRI, histologically, and immunochemically for Periods 1 (Figure 5 A–D) and 2 (Figure 5E–H). LDLs from the cis-MUFA control groups had the greatest enrichment in CO, followed by the n-3 PUFA fed mice and the SOAT2 ASO treated mice (Figure 5A and 5E). Atherosclerosis measurements by each method mirrored the degree of enrichment of the LDL in CO. For Period 1, the cis-MUFA fed mice had larger wall areas, intimal areas and more CE deposition into the abdominal aorta compared to the n-3 PUFA fed mice. A step-wise decrease in atherosclerosis burden was observed after Period 2 with the cis-MUFA control mice having the most severe burden followed by the n-3 PUFA fed mice and the SOAT2 ASO treated mice.

DISCUSSION

This is the first study to show the importance of SOAT2 in the treatment of established atherosclerosis. Here, we extend earlier work to show that gene knockdown of hepatic SOAT2 attenuates CO packaging into LDL; this compositional modification was associated with less aortic atherosclerosis, which was measured by MRI, histology, and chemically. SOAT2 treatment caused a striking reversal of aortic wall area over the final four weeks of treatment (Figure 2D) suggesting lesion size regression. Lesions contained 10-fold less lipid and nearly three times more collagen content compared to lesions from mice sacrificed at baseline in Period 2 (Figure 3B, 3C). Both findings are consistent with favorable remodeling of lesions to a more stable phenotype[15, 16].

Because MR images were captured at the end of systole during maximum blood flow to eliminate signal from the blood, measurements of the same sections were consistently larger on MR than when measured histologically where sections were obtained from flaccid vessels at post mortem. Additionally, vessels shrink after removal from the body and during histological preparation[17–19], and storage at low temperatures may exacerbate this phenomenon. A combination of all of these factors likely caused the quantitative differences observed between MR images and histology; a finding consistent with previous studies comparing these techniques[20, 21]. However, the consistency of these differences across all experimental groups and the strong relationships with histological data indicate the MRI technique was an accurate and sensitive tool for monitoring wall morphology and changes associated with disease development and treatment.

Both n-3 PUFA and SOAT2 ASO treatments arrested CE deposition into the artery wall (Figure 3D); however, we observed an increase in arterial FC content in both experimental groups. This is consistent with regression studies in both non-human primates[22] and mice[23] which reported that early stages of plaque regression were accompanied by robust decreases in arterial CE and foam cells with concomitant increases in FC. In the current study

abdominal FC:CE was highest in the SOAT2 ASO treated mice (1.6) compared to the n-3 PUFA and cis-MUFA experimental groups (~1.0). Additionally, MRI measurements show rapid decreases in the wall area exclusively in the SOAT2 ASO group contained to the final four weeks of the study. Taken together, this suggests that the SOAT2 ASO treatment group was still in the earlier stages of lesion repair.

The benefits of hepatic SOAT2 knockdown were observed in the apoB100-only, LDLr$^{-/-}$ mouse model, with high circulating levels of LDL. This model was chosen because it is reflective of the lipoprotein distribution seen in humans. The 24-week atherogenic diet challenge in Period 1 exacerbated the size, complexity, and severity of the plaques in the aorta. Furthermore, mice received the SOAT2 treatment while still consuming the atherogenic diet, mimicking the typical human diet. This makes this study translationally relevant considering that in humans, atherosclerosis begins in early childhood[24] and thus therapeutic approaches to reverse vulnerable plaque formation are highly desired.

Recently, we have shown that cholesterol esters derived from hepatic SOAT2 are associated with more severe atherosclerosis than those from the intestine[25] in LDLr$^{-/-}$ mice. This was found despite lower SOAT2 activity levels in the liver compared to the intestine of these mice. The current study used an ASO to specifically target SOAT2 in the liver. This ASO has been previously characterized and used in multiple studies[10, 26, 27]. It is highly specific to hepatic SOAT2 and results in no observable liver toxicity or non-specific effects on intestinal SOAT2 or SOAT1 activity levels[10]. Results from this study suggest that pharmacologic intervention to knockdown SOAT2 in the liver is effective for remodeling atherosclerotic lesions into a more stable phenotype. Importantly, SOAT2 is the major cholesterol-esterifying enzyme in human liver. Furthermore, it appears that SOAT2 activity levels in humans recapitulate what we recently reported in the LDLr$^{-/-}$ mouse[25] with humans having low hepatic SOAT2 activity[28] relative to intestinal SOAT2 activity[29]. We have shown that intestinal depletion of SOAT2 effectively blocks cholesterol ester accumulation in the liver and plasma[30]; however, further investigation is needed to determine whether inhibition of SOAT2 at the intestinal level provides the same benefit for preexisting disease.

SOAT2 ASO-treated mice had a 44% reduction in plasma HDL cholesterol. This is paradoxical as HDL is generally accepted to play a critical role in the removal excess arterial cholesterol via reverse cholesterol transport. However, HDL is a heterogenous population of particles,[31] and different populations have different functions[32]. A previous report using the same SOAT2 ASO in mice found that reduction of hepatic SOAT2 activity resulted in a redistribution of plasma cholesterol into larger HDL particles[27]. The authors characterized the particle population showing it was enriched in both apolipoproteins A–I and E and, importantly, had increased cholesterol efflux capacity. Interestingly, this was only observed when the western-type diet was started prior to the SOAT2 ASO intervention like the present study. Thus, it's reasonable that while we observed a decrease in total plasma HDL cholesterol, there was an increase in this subpopulation of HDL that promotes cholesterol efflux out of the artery wall. This is translationally relevant as HDL cholesterol is inversely correlated to SOAT2 activity[33] and SOAT2 has been identified as a candidate gene that impacts HDL levels in humans[34]

Circulating levels of apoB-containing lipoproteins, particularly LDL, are important in the initiation and development of atherosclerosis[5] thus it makes sense that robust reductions in LDL are required for plaque regression. Both SOAT2 treatment and dietary intervention with n-3 PUFAs resulted in marked reductions in circulating levels of LDL. However, favorable remodeling of the lesion was only observed in the SOAT2 ASO treatment group suggesting that lowering LDL alone is not sufficient to achieve plaque regression. Several mechanisms could be responsible for the benefits of SOAT2 knockdown. The primary difference observed between the SOAT2 ASO and n-3 PUFA groups in the current study was in the compositional modification of the LDL CEs. Consistent with our previous studies, SOAT2 knockdown was the most effective at reducing CO packaging in LDL. Previously we have shown that LDLs with less CO have a decreased affinity for binding to arterial proteoglycans and thus being retained in the artery wall which was protective against the development of atherosclerosis[14]. In addition, evidence in a different mouse model of atherosclerosis suggests that LDLs depleted in CO are less susceptible to aggregation (Oomi K, Rudel LL, unpublished data). It is likely a combination of factors lead to the beneficial outcome associated with SOAT2 knockdown in this study. While work remains to elucidate the specific mechanism(s) responsible for these results, our findings suggest that SOAT2 is a viable therapeutic target for treatment of atherosclerosis.

Supplementary Material

Refer to Web version on PubMed Central for supplementary material.

Acknowledgments

We thank Richard Lee, Mark Graham, and Rosanne Crooke for generously providing the SOAT2 ASO used in this study. Additionally, we thank Josh Tan for technical assistance in MR image acquisition and processing, Cathy Mathis for her guidance on tissue sectioning, Karen Klein for her help editing the manuscript and Hermina Borgerink for performing histological staining. The mass spectrometry core lab run by Dr. Michael Thomas and Mike Samuels (Wake Forest School of Medicine, Biochemistry Department) performed mass spectrometry analyses on the LDL particle cholesterol esters within LDL particles.

SOURCES OF FUNDING

This work was partially supported by the Center for Biomolecular Imaging and by P01 HL49373 (Lawrence Rudel, PI), and T32HL091797 (John Parks, PI), from which JTM received a predoctoral stipend.

Nonstandard Abbreviations and Acronyms

apoB	apolipoprotein B
ASO	antisense oligonucleotide
CE	cholesterol ester
CHD	coronary heart disease
Cis-MUFA	cis-mono unsaturated fatty acid
CO	cholesterol oleate
EEL	external elastic lamina

FA	flip angle
FC	free cholesterol
FLASH	fast low angle shot
FOV	field of view
HDL	high-density lipoprotein
IEL	internal elastic lamina
LDL	low-density lipoprotein
MRI	magnetic resonance imaging
MT	masson's trichrome
n-3 PUFA	n-3 polyunsaturated fatty acid
NBF	neutral buffered formalin
NEX	number of excitations
ORO	oil-red O
PBS	phosphate buffered saline
PL	phospholipid
PRO	protein
RF	radio frequency
SOAT2	sterol-O-acyltransferase 2
TE	excitation time
TG	triglyceride
TPC	total plasma cholesterol
TR	relaxation time
VLDL	very low-density lipoprotein
VVG	Verhoeff-Van Gieson

References

1. Farmer JA, Gotto AM Jr. Dyslipidemia and the vulnerable plaque. Prog Cardiovasc Dis. 2002; 44:415–428. [PubMed: 12077715]
2. Davies MJ. The composition of coronary-artery plaques. N Engl J Med. 1997; 336:1312–1314. [PubMed: 9113937]
3. Nissen SE, Tuzcu EM, Schoenhagen P, Brown BG, Ganz P, Vogel RA, Crowe T, Howard G, Cooper CJ, Brodie B, Grines CL, DeMaria AN. Effect of intensive compared with moderate lipid-lowering therapy on progression of coronary atherosclerosis: A randomized controlled trial. JAMA. 2004; 291:1071–1080. [PubMed: 14996776]
4. Nissen SE, Nicholls SJ, Sipahi I, Libby P, Raichlen JS, Ballantyne CM, Davignon J, Erbel R, Fruchart JC, Tardif JC, Schoenhagen P, Crowe T, Cain V, Wolski K, Goormastic M, Tuzcu EM.

Effect of very high-intensity statin therapy on regression of coronary atherosclerosis: The asteroid trial. JAMA. 2006; 295:1556–1565. [PubMed: 16533939]

5. Williams KJ, Feig JE, Fisher EA. Rapid regression of atherosclerosis: Insights from the clinical and experimental literature. Nat Clin Pract Card. 2008; 5:91–102.
6. Ma J, Folsom AR, Lewis L, Eckfeldt JH. Relation of plasma phospholipid and cholesterol ester fatty acid composition to carotid artery intima-media thickness: The atherosclerosis risk in communities (aric) study. Am J Clin Nutr. 1997; 65:551–559. [PubMed: 9022543]
7. Warensjo E, Sundstrom J, Vessby B, Cederholm T, Riserus U. Markers of dietary fat quality and fatty acid desaturation as predictors of total and cardiovascular mortality: A population-based prospective study. Am J Clin Nutr. 2008; 88:203–209. [PubMed: 18614742]
8. Rudel LL, Johnson FL, Sawyer JK, Wilson MS, Parks JS. Dietary polyunsaturated fat modifies low-density lipoproteins and reduces atherosclerosis of nonhuman primates with high and low diet responsiveness. Am J Clin Nutr. 1995; 62:463S–470S. [PubMed: 7625361]
9. Rudel LL, Parks JS, Sawyer JK. Compared with dietary monounsaturated and saturated fat, polyunsaturated fat protects african green monkeys from coronary artery atherosclerosis. Arterioscler Thromb Vasc Biol. 1995; 15:2101–2110. [PubMed: 7489230]
10. Bell TA 3rd, Brown JM, Graham MJ, Lemonidis KM, Crooke RM, Rudel LL. Liver-specific inhibition of acyl-coenzyme a:Cholesterol acyltransferase 2 with antisense oligonucleotides limits atherosclerosis development in apolipoprotein b100-only low-density lipoprotein receptor−/− mice. Arterioscler Thromb Vasc Biol. 2006; 26:1814–1820. [PubMed: 16675724]
11. Bell TA 3rd, Kelley K, Wilson MD, Sawyer JK, Rudel LL. Dietary fat-induced alterations in atherosclerosis are abolished by acat2-deficiency in apob100 only, ldlr−/− mice. Arterioscler Thromb Vasc Biol. 2007; 27:1396–1402. [PubMed: 17431188]
12. Rudel LL, Kelley K, Sawyer JK, Shah R, Wilson MD. Dietary monounsaturated fatty acids promote aortic atherosclerosis in ldl receptor-null, human apob100-overexpressing transgenic mice. Arterioscler Thromb Vasc Biol. 1998; 18:1818–1827. [PubMed: 9812923]
13. VanderLaan PA, Reardon CA, Getz GS. Site specificity of atherosclerosis: Site-selective responses to atherosclerotic modulators. Arterioscler Thromb Vasc Biol. 2004; 24:12–22. [PubMed: 14604830]
14. Melchior JT, Sawyer JK, Kelley KL, Shah R, Wilson MD, Hantgan RR, Rudel LL. Ldl particle core enrichment in cholesteryl oleate increases proteoglycan binding and promotes atherosclerosis. J Lipid Res. 2013; 54:2495–2503. [PubMed: 23804810]
15. Brown BG, Zhao XQ, Sacco DE, Albers JJ. Atherosclerosis regression, plaque disruption, and cardiovascular events: A rationale for lipid lowering in coronary artery disease. Annu Rev Med. 1993; 44:365–376. [PubMed: 8476257]
16. Aikawa M, Rabkin E, Okada Y, Voglic SJ, Clinton SK, Brinckerhoff CE, Sukhova GK, Libby P. Lipid lowering by diet reduces matrix metalloproteinase activity and increases collagen content of rabbit atheroma: A potential mechanism of lesion stabilization. Circulation. 1998; 97:2433–2444. [PubMed: 9641696]
17. Cilingiroglu M, Oh JH, Sugunan B, Kemp NJ, Kim J, Lee S, Zaatari HN, Escobedo D, Thomsen S, Milner TE, Feldman MD. Detection of vulnerable plaque in a murine model of atherosclerosis with optical coherence tomography. Catheter Cardiovasc Interv. 2006; 67:915–923. [PubMed: 16602128]
18. Jahnke C, Dietrich T, Paetsch I, Koehler U, Preetz K, Schnackenburg B, Fleck E, Graf K, Nagel E. Experimental evaluation of the detectability of submillimeter atherosclerotic lesions in ex vivo human iliac arteries with ultrahigh-field (7.0 t) magnetic resonance imaging. Int J Cardiovasc Imaging. 2007; 23:519–527. [PubMed: 17109199]
19. Johnstone MT, Botnar RM, Perez AS, Stewart R, Quist WC, Hamilton JA, Manning WJ. In vivo magnetic resonance imaging of experimental thrombosis in a rabbit model. Arterioscler Thromb Vasc Biol. 2001; 21:1556–1560. [PubMed: 11557688]
20. Fayad ZA, Fallon JT, Shinnar M, Wehrli S, Dansky HM, Poon M, Badimon JJ, Charlton SA, Fisher EA, Breslow JL, Fuster V. Noninvasive in vivo high-resolution magnetic resonance imaging of atherosclerotic lesions in genetically engineered mice. Circulation. 1998; 98:1541–1547. [PubMed: 9769308]

21. Yuan C, Beach KW, Smith LH Jr, Hatsukami TS. Measurement of atherosclerotic carotid plaque size in vivo using high resolution magnetic resonance imaging. Circulation. 1998; 98:2666–2671. [PubMed: 9851951]
22. Small DM, Bond MG, Waugh D, Prack M, Sawyer JK. Physicochemical and histological changes in the arterial wall of nonhuman primates during progression and regression of atherosclerosis. J Clin Invest. 1984; 73:1590–1605. [PubMed: 6725553]
23. Potteaux S, Gautier EL, Hutchison SB, van Rooijen N, Rader DJ, Thomas MJ, Sorci-Thomas MG, Randolph GJ. Suppressed monocyte recruitment drives macrophage removal from atherosclerotic plaques of apoe−/− mice during disease regression. J Clin Invest. 2011; 121:2025–2036. [PubMed: 21505265]
24. Freedman DS, Newman WP 3rd, Tracy RE, Voors AE, Srinivasan SR, Webber LS, Restrepo C, Strong JP, Berenson GS. Black-white differences in aortic fatty streaks in adolescence and early adulthood: The bogalusa heart study. Circulation. 1988; 77:856–864. [PubMed: 3258194]
25. Zhang J, Sawyer JK, Marshall SM, Kelley KL, Davis MA, Wilson MD, Brown JM, Rudel LL. Cholesterol esters derived from hepatic sterol o-acyltransferase 2 are associated with more atherosclerosis than ce from intestinal soat2. Circ Res. 2014; 115:826–833. [PubMed: 25239141]
26. Brown JM, Bell TA 3rd, Alger HM, Sawyer JK, Smith TL, Kelley K, Shah R, Wilson MD, Davis MA, Lee RG, Graham MJ, Crooke RM, Rudel LL. Targeted depletion of hepatic acat2-driven cholesterol esterification reveals a non-biliary route for fecal neutral sterol loss. J Biol Chem. 2008; 283:10522–10534. [PubMed: 18281279]
27. Pedrelli M, Davoodpour P, Degirolamo C, Gomaraschi M, Graham M, Ossoli A, Larsson L, Calabresi L, Gustafsson JA, Steffensen KR, Eriksson M, Parini P. Hepatic acat2 knock down increases abca1 and modifies hdl metabolism in mice. PLoS One. 2014; 9:e93552. [PubMed: 24695360]
28. Parini P, Davis M, Lada AT, Erickson SK, Wright TL, Gustafsson U, Sahlin S, Einarsson C, Eriksson M, Angelin B, Tomoda H, Omura S, Willingham MC, Rudel LL. Acat2 is localized to hepatocytes and is the major cholesterol-esterifying enzyme in human liver. Circulation. 2004; 110:2017–2023. [PubMed: 15451793]
29. Jiang ZY, Jiang CY, Wang L, Wang JC, Zhang SD, Einarsson C, Eriksson M, Han TQ, Parini P, Eggertsen G. Increased npc1l1 and acat2 expression in the jejunal mucosa from chinese gallstone patients. Biochem Biophys Res Commun. 2009; 379:49–54. [PubMed: 19071091]
30. Zhang J, Kelley KL, Marshall SM, Davis MA, Wilson MD, Sawyer JK, Farese RV Jr, Brown JM, Rudel LL. Tissue-specific knockouts of acat2 reveal that intestinal depletion is sufficient to prevent diet-induced cholesterol accumulation in the liver and blood. J Lipid Res. 2012; 53:1144–1152. [PubMed: 22460046]
31. Gordon SM, Deng J, Lu LJ, Davidson WS. Proteomic characterization of human plasma high density lipoprotein fractionated by gel filtration chromatography. J Proteome Res. 2010; 9:5239–5249. [PubMed: 20718489]
32. Camont L, Chapman MJ, Kontush A. Biological activities of hdl subpopulations and their relevance to cardiovascular disease. Trends Mol Med. 2011; 17:594–603. [PubMed: 21839683]
33. Parini P, Jiang ZY, Einarsson C, Eggertsen G, Zhang SD, Rudel LL, Han TQ, Eriksson M. Acat2 and human hepatic cholesterol metabolism: Identification of important gender-related differences in normolipidemic, non-obese chinese patients. Atherosclerosis. 2009; 207:266–271. [PubMed: 19467657]
34. Qiu S, Luo S, Evgrafov O, Li R, Schroth GP, Levitt P, Knowles JA, Wang K. Single-neuron rna-seq: Technical feasibility and reproducibility. Front Genet. 2012; 3:124. [PubMed: 22934102]

SIGNIFICANCE

Studies in humans and animal models indicate SOAT2 promotes development of coronary heart disease by packaging cholesterol oleate into circulating apoB-containing lipoproteins. Inhibition of SOAT2 has been shown to protect against the development of atherosclerosis but studies inhibiting SOAT2 to evaluate atheroma regression are limited. The current study induces complex arterial lesions which mimic vulnerable, fatty lesions in humans by feeding a diet enriched in monounsaturated fat, “the healthy fat”, in a mouse model of human atherosclerosis. We used an antisense oligonucleotide to knockdown expression of SOAT2 in the liver and evaluated the effects on the arterial lesions. We found that gene knockdown of SOAT2 inhibits packaging of cholesterol oleate in apoB-containing lipoproteins and results in a favorable remodeling of the plaques to a stable phenotype indicating SOAT2 is an important target for treatment of established atherosclerosis.

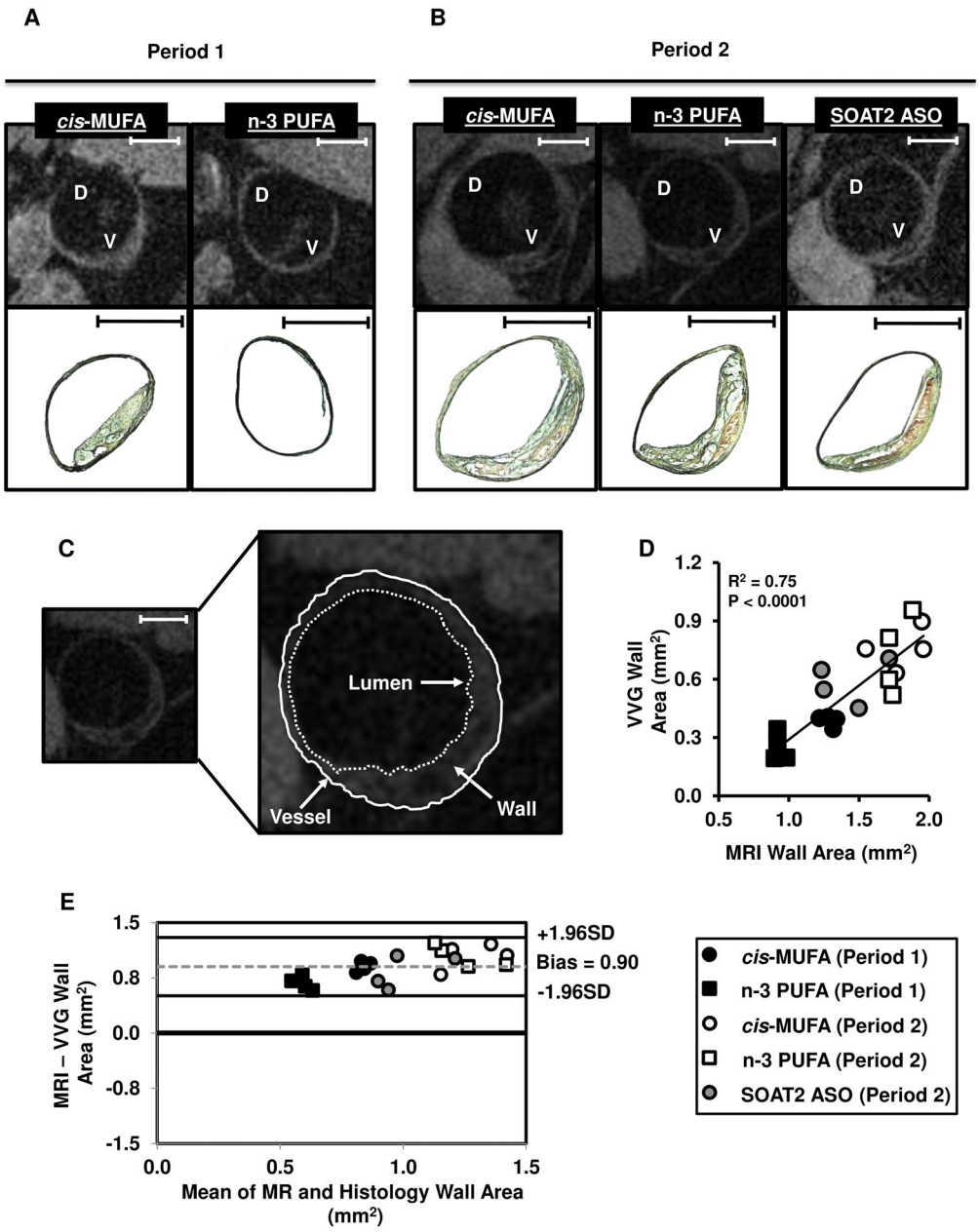

Figure 1. Aortic arch measurements using MRI and histology

Transverse images of the aortic arch obtained by MRI (top row) and Verhoeff-van Gieson-stained histological sections (bottom row) at the end of Period 1 (**A**) and Period 2 (**B**). **C:** Sample image showing how vessel wall components were delineated for MRI measurements. (**D**) and (**E**): Relationships between MRI and histological measurements of cross-sectional wall area are shown by regression analysis and a Bland-Altman plot, respectively. Within images, D indicates dorsal and V indicates ventral. Bars = 1 mm.

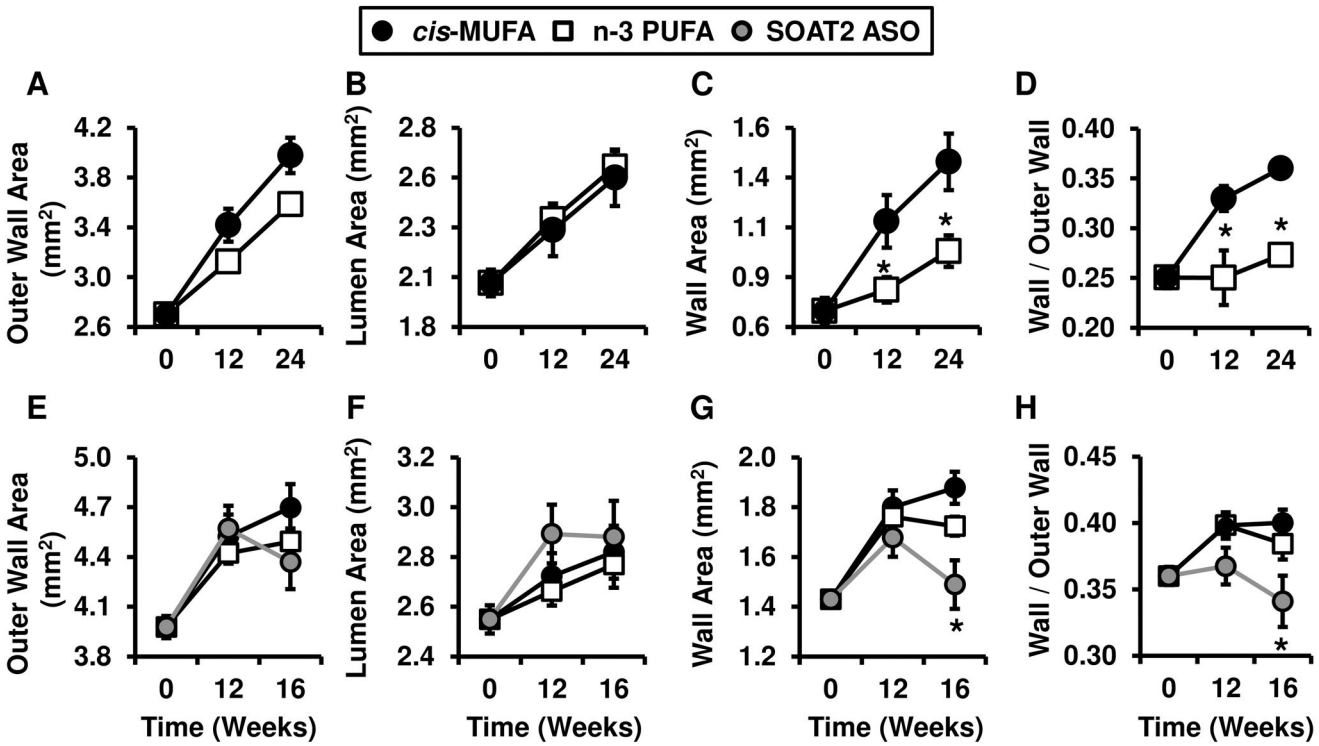

Figure 2. Changes in aortic arch as evaluated by MRI

Vessel area, lumen area, wall area, and ratio of wall/vessel as obtained by MRI shown at each time point for Period 1 (**A–D**) and Period 2 (**E–F**). Bars indicate means (±SEM) for n ≥4 mice in each experimental group. Asterisks indicate a statistically significant difference from cis-MUFA-fed group within each time point; $P<0.05$ by Tukey's honestly significant difference.

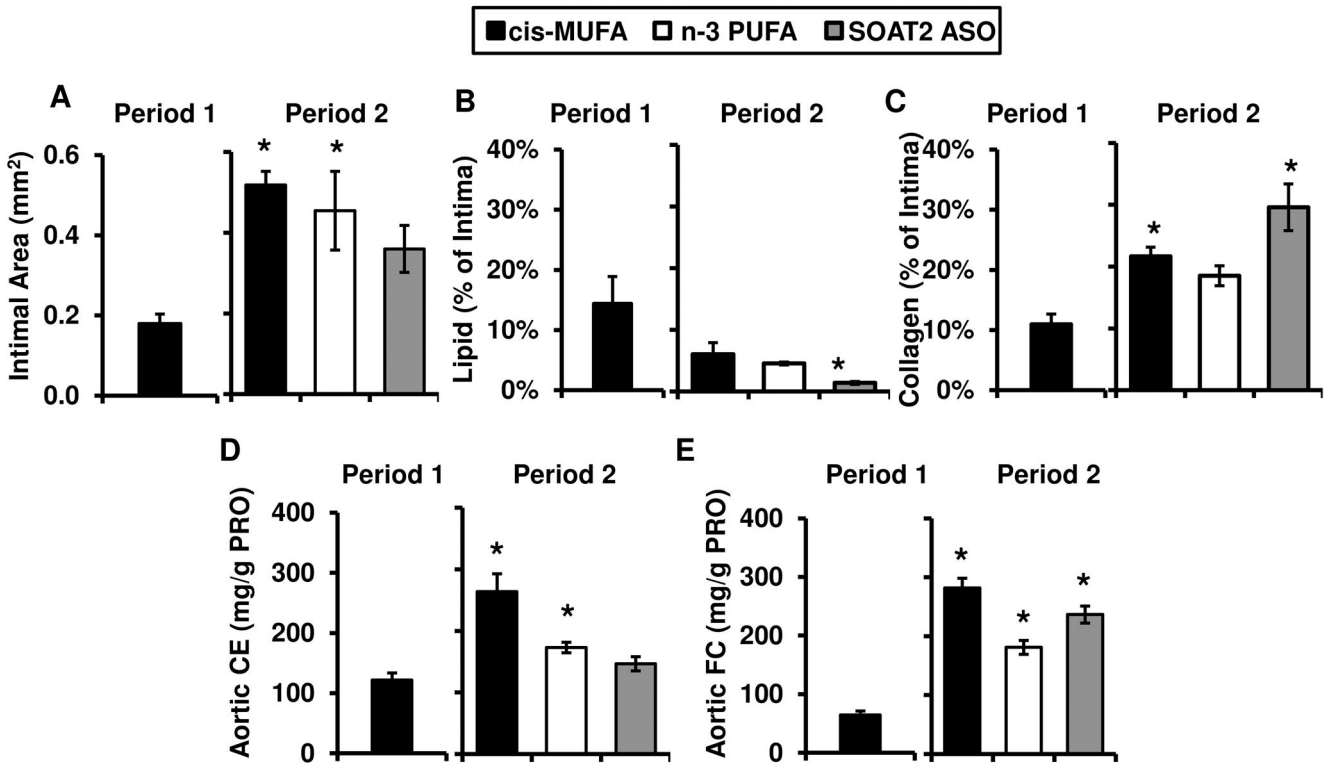

Figure 3. Effects of diet and SOAT2 knockdown on atherosclerosis

A: Histologic measurement of intimal area obtained by Verhoeff-van Gieson staining of sections. **B** and **C:** Lipid and collagen content, each expressed as a percentage of intimal area. Bars indicate means (±SEM) for n = 4 mice for each experimental group. **D, E:** Cholesterol ester (CE) and free cholesterol (FC) deposition in the abdominal aorta. Bars represent means (±SEM) for n = 7–11 mice for each experimental group. One-way analysis of variance with a Dunnet's correction was used to determine statistically significant differences between the cis-MUFA-fed mice in Period 1 and groups from Period 2. Asterisks denote statistically significant differences at $P<0.05$.

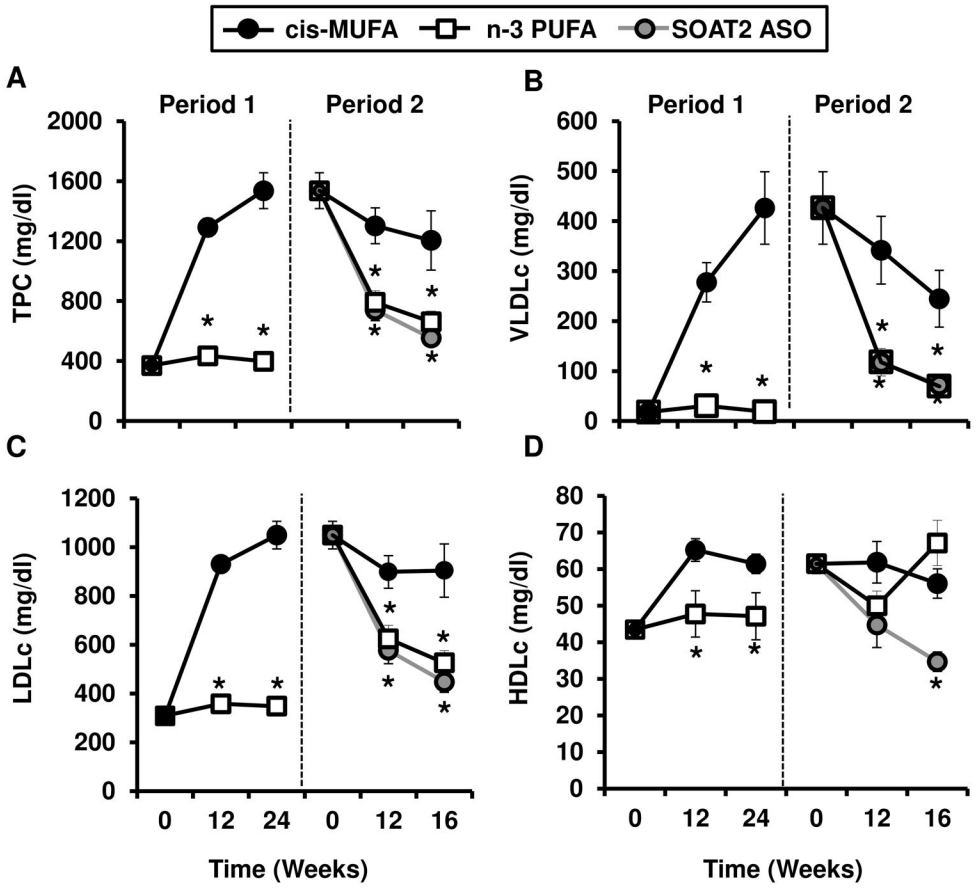

Figure 4. Effects of diet and SOAT2 knockdown on plasma cholesterol concentrations

(A): Total plasma cholesterol (TPC) concentrations determined at each time point by enzymatic assay. Cholesterol distribution among lipoprotein classes at each time point (**B–D**) was determined after gel filtration chromatography to separate lipoprotein classes. Bars indicate means (±SEM) for n≥5 mice per experimental group at each time point. Asterisks indicate a statistically significant difference from cis-MUFA fed experimental mice (black circles) within each time point with $P<0.05$ by Tukey's honestly significant difference. HCLc, high-density lipoprotein cholesterol; LDLc, low-density lipoprotein cholesterol; VLDLc, very low-density lipoprotein cholesterol.

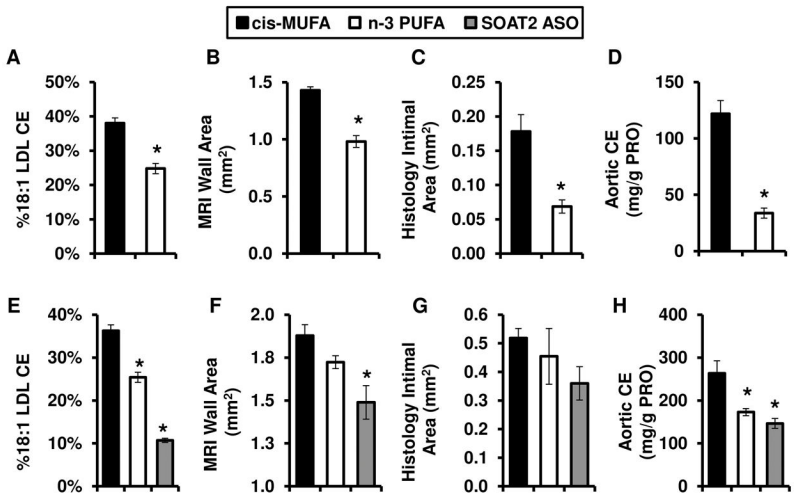

Figure 5. Relationships between atherosclerosis and LDL cholesterol oleate

LDL cholesterol oleate content (%18:1 LDL CE), MRI wall area, histological intimal area, and aortic cholesterol ester content for Period 1 (**A–D**, respectively) and Period 2 (**E–H**, respectively). Bars indicate means (±SEM) for n=5 mice in each experimental group for LDL cholesterol oleate, n=4–6 mice in each experimental group for wall area, n=4 mice in each experimental group for intimal area, and n≥9 mice in each experimental group for aortic CE content. One-way analysis of variance with a Dunnet's correction was used to determine statistically significant differences between the cis-MUFA-fed mice and other groups. Asterisks denote statistically significant differences at $P<0.05$.

Table 1

Cholesterol Esters Expressed as Percentage of Total CE Fraction in LDL, Determined by Mass Spectrometry

	Phase Diet Tx	Period 1		Period 2		
		cis-MUFA	n-3 PUFA	cis-MUFA	n-3 PUFA	cis-MUFA SOAT2 ASO
Cholesteryl Esters, wt %	C16:0	5.8 (0.2)	7.8 ¶ (0.1)	5.5 (0.1)	6.4 ¶ (0.2)	3.5 ¶ (0.1)
	C18:0	1.1 (0.2)	1.1 (0.1)	0.7 ¶ (0.1)	0.9 (0.1)	0.2 ¶ (0.1)
	C16:1	12.6 (0.6)	22.6 ¶ (0.7)	12.9 (0.8)	16.4 ¶ (0.2)	3.8 ¶ (0.5)
	C18:1	38.0 (1.6)	24.8 ¶ (1.5)	36.3 (1.4)	25.4 ¶ (1.2)	10.7 ¶ (0.5)
	C18:2	15.4 (0.6)	8.1 ¶ (0.5)	15.1 (0.6)	7.1 ¶ (0.1)	21.5 ¶ (1.8)
	C20:4	20.5 (1.7)	8.2 ¶ (0.5)	22.2 (2.2)	9.0 ¶ (0.3)	46.7 ¶ (2.7)
	C18:3	0.7 (0.1)	1.2 ¶ (0.1)	0.7 (0.0)	0.9 (0.0)	1.0 ¶ (0.1)
	C20:5	1.5 (0.2)	20.3 ¶ (1.2)	1.9 (0.1)	26.2 ¶ (1.0)	2.2 (0.2)
	C22:6	4.3 (0.3)	5.8 (0.3)	4.8 (0.3)	7.7 ¶ (0.5)	10.4 ¶ (0.7)

All values represent the means (± SEM) for 5 mice for each experimental group. Values in a column with symbols are significantly different at $P<0.05$ from the cis-MUFA mice at the end of Period 1 (first column) as determined by a one-way analysis of variance with a Dunnet's correction. Percentages of palmitic acid (C16:0), stearic acid (C18:0), palmitioleic acid (C16:1), oleic acid (C18:1), linoleic acid (C18:2), arachidonic acid (C20:4), α-linoleic acid (C18:3), eicosapentaenoic acid (C20:5), and docosahexaenoic acid (C22:6).